3D processing maps and a modified constitutive model of 16Cr-5Ni-Mo supermartensitic stainless steel

3D processing maps and a modified constitutive model of 16Cr-5Ni-Mo supermartensitic stainless steel

Y W Sun*, Y P Zhong, L S Wang and F X Fan
Luoyang Ship Material Research Institute, Luoyang 471000, China
*E-mail: weiyong09@163.com

Abstract. The hot deformation behavior of 16Cr-5Ni-Mo supermartensitic stainless steel was investigated using a Gleeble-1500D thermo-mechanical simulator in the temperature range of 850 to 1150℃ and strain rate range of 0.01 to 10 s^{-1}. The hot deformation apparent activation energy of the steel was obtained as 424.173 kJ/mol. Arrhenius type constitutive equation was established according to flow stress data to describe the flow behavior. Meanwhile, the 3D maps of power dissipation and processing based on dynamic materials mode (DMM) were developed for the typical strains of 0.2, 0.4, 0.6 and 0.8, respectively. The results show that with the high deformation temperature (1000-1150℃) and low strain rate (0.01—0.1 s^{-1}), it is dominated by the dynamic recrystallization (DRX) for the softening mechanism. And the critical strains for the onset of DRX at different conditions are obtained. The optimized processing parameters for hot working of 16Cr-5Ni-Mo supermartensitic stainless steel are in the temperature range of 980—1150℃ and strain rate range of 0.02—0.36 s^{-1} at strains of 0.6 and 0.8.

1. Introduction

Supermartensitic stainless steels are widely used as structural components in applications such as impeller blade [1], propeller blade bolts [2], power plant [3], high strength fasteners served in the marine environment, and so on. These steels have excellent mechanical properties, good corrosion resistance, good fatigue property, and excellent weldability [4-5]. And they can be used as bars, sheets, and forged parts. 16Cr-5Ni-Mo steel is a low-carbon supermartensitic stainless steel containing less than 0.05 wt.% C. The steel is strengthened by the solution treatment and lath martensite transformation. Recently, some high strength 16Cr-5Ni-Mo steel fasteners used as 12.9 grade are serving in safety in marine engineering equipment. Due to the excellent corrosion resistance, high strength, and toughness, the need of 16Cr-5Ni-Mo is huge in the future market. However, some defects often occur during the forging of products resulting in the waste of time and economic cost. Hot deformation behavior research of steels that usually conducted in the stability range corresponding to the single austenite phase plays an essential role in hot working for the production of parts [6], and it is necessary to study the constitutive models and processing maps of the steel.

Recently, the investigations of hot deformation are focused on the aluminum alloys, magnesium alloys, copper alloys, titanium alloys, alloy steel, superalloy, and duplex stainless steel, etc. [7-10]. The hot deformation of supermartensitic stainless steels has been fewer reported in recent years, especially on the aspect of the onset of DRX. And it is vital that these steels don't have perfect hot workability due to the harmful phase under the high temperature. The investigation of 16Cr-5Ni-Mo supermartensitic stainless steel should be paid attention to the hot deformation behavior which is primarily used as an essential engineering material. In this study, the effects of deformation strain, temperature, and strain rate on the hot deformation behavior of 16Cr-5Ni-Mo steel are investigated while the typical Arrhenius model constitutive equation is also established. It is noted that in this work, three-dimensional (3D) maps are developed to instruct the hot deformation process and provide the optimum hot working parameters. Therefore, the present work is helpful in solving the problems of 16Cr-5Ni-Mo steel during practical production.

2. Materials and Experimental Procedures

The chemical compositions of the 16Cr-5Ni-Mo supermartensitic stainless steel used in this work are shown in table 1. The steel was supplied with a diameter of 95 mm bar, which was prepared by vacuum induction melting and electroslag remelting. Then, the ingots were forged to obtain the homogeneous microstructure and reduce the defects.

Hot compression tests of the 16Cr-5Ni-Mo steel were carried out on a Gleeble-1500D thermo-mechanical simulator at the temperature of 850, 900, 1000, 1100 and 1150 ℃ with strain rates of 0.01, 0.1, 1 and 10 s^{-1}, respectively. Before each test, the sample was maintained at the solution temperature of 1150 ℃ to achieve a stable microstructure. Every sample was hot compressed to a total true strain of 0.9. And all the samples were quenched in water quickly after hot deformation to preserve the deformed microstructure.

The compressed samples were sectioned parallel to the compression axis and polished according to the standard procedure and then etched with a solution of 5g $FeCl_3$, 10 ml HCl and 50 ml H_2O. And then the microstructures were observed using ZEISS Observer. Zim optical microscopy.

Table 1.Chemical compositions of 16Cr-5Ni-Mosupermartensitic stainless steel used in this study (wt%)

C	Si	Mn	S	P	H	N	O	Al	Cr	Ni	Mo
0.04	0.50	0.80	0.0016	0.0076	0.00017	0.028	0.0023	<0.010	16.08	4.43	1.34

3. Results and Discussion

3.1. Constitutive equation of 16Cr-5Ni-Mo steel

Constitutive equations are often used to predict the resistance to deformation of materials during forging, rolling and so on. In this study, the class Arrhenius constitutive equations [11] can be summarized with the deformation parameters of flow stress σ, deformation temperature T and strain rate $\dot{\varepsilon}$:

$$\dot{\varepsilon} = A_1\sigma^{n'}\exp(-Q/RT) \qquad (\alpha\sigma<0.8, \text{ low stress}) \tag{1}$$

$$\dot{\varepsilon} = A_2\exp(\beta\sigma)\exp(-Q/RT) \qquad (\alpha\sigma>1.2, \text{ high stress}) \tag{2}$$

$$\dot{\varepsilon} = A[\sinh(\alpha\sigma)]^n\exp(-Q/RT) \qquad (\text{for all stress}) \tag{3}$$

where A_1, A_2, A, α, β, n, n', and β represent material constants; Q is the apparent activation energy, which is described as the degree of difficulty for deformation; the value of R is 8.314 $J\cdot mol^{-1}\cdot K^{-1}$; T is Kelvin temperature. And the value of α is calculated by [12]: $\alpha = \beta/n'$.

Furthermore, the influence of strain rate and temperature on the hot deformation behaviors can be described by the Zener-Hollomon parameter Z [13], which is shown in equation (4). And then substituting equation (3) into equation (4) gives equation (5).

$$Z = \dot{\varepsilon} \exp[\frac{Q}{RT}] \tag{4}$$

$$Z = A[\sinh(\alpha\sigma)]^n \tag{5}$$

With the natural logarithms based on Equations. (1), (2) and (5), the material constants and apparent activation energy are obtained as follows:

$$\ln \dot{\varepsilon} = \ln A_1 - \frac{Q}{RT} + n' \ln \sigma \tag{6}$$

$$\ln \dot{\varepsilon} = \ln A_2 - \frac{Q}{RT} + \beta\sigma \tag{7}$$

$$\ln Z = \ln A + n \ln[\sinh(\alpha\sigma)] \tag{8}$$

In this research, the true stress at the total strain of 0.9 is used for the above linear regression analysis to determine the relevant parameters of the 16Cr-5Ni-Mo steel. The relationship among $\dot{\varepsilon}$, σ and T of the steel is illustrated in figure1. The value of n' can be obtained from the slope of ln(strain rate)-lnσ at the temperature of 1150℃, while β is determined from the slope of ln(strain rate)-σ at the temperature of 850℃. For the certain temperature and strain rate, the apparent activation energy Q is expressed as:

$$Q = R\frac{\partial \ln[\sinh(\alpha\sigma)]}{\partial(1/T)}\bigg|_{\dot{\varepsilon}} \frac{\partial \ln \dot{\varepsilon}}{\partial \ln[\sinh(\alpha\sigma)]}\bigg|_T = RS_1S_2 \tag{9}$$

From figure1(c) and (d), the slopes of ln[sinh($\alpha\sigma$)]-1/T and ln(strain rate)-ln[sinh($\alpha\sigma$)] is obtained on average. And the values of S_1 and S_2 are 5.028 and 10.147, respectively. The values of the 16Cr-5Ni-Mo steel constants during hot deformation can be calculated as follows: n'=6.2343, β=0.0677, α=0.011, n=4.985, ln$A$=33.510, Q=424.173 kJ/mol. Therefore, based on the above experimental data and model, the Arrhenius constitutive equation of the steel can be expressed as follows:

$$\dot{\varepsilon} = 3.57 \times 10^{14}[\sinh(0.011\sigma)]^{4.985} \exp(-\frac{424173}{RT}) \tag{10}$$

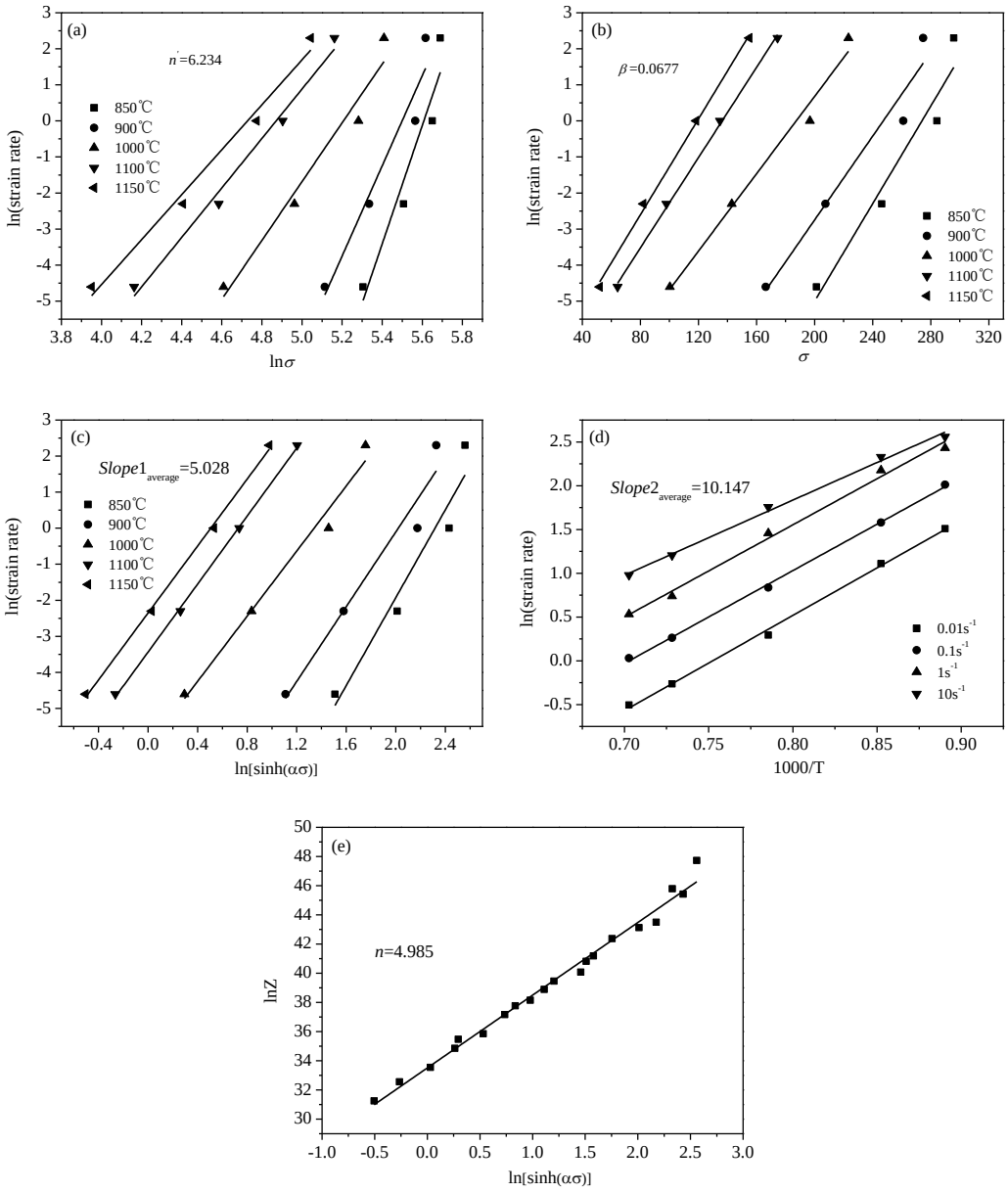

Figure 1 Relationships between temperature, peak stress and strain rate of 16Cr-5Mo-Ni steel: (a) ln(strain rate)-lnσ;(b) ln(strain rate)-σ; (c) ln(strain rate)-ln[sinh($\alpha\sigma$)]; (d) ln[sinh($\alpha\sigma$)]-1/T; (e) ln[sinh($\alpha\sigma$)]-ln$Z$

3.2. Constitutive models considering dynamic recrystallization (DRX) of 16Cr-5Ni-Mo steel

In above investigations, using of Arrhenius mode constitutive equation has been the common modeling approach for predicting the deformation parameters during hot deformation. However, the model consists of a few material constants, which can derive from the hot compression tests. And it is important that the influence of dislocation mechanism is ignored in the above equation. During the deformation, the dislocation mechanism plays an important role on the DRX. Hence, it is necessary to establish a model considering the DRX of 16Cr-5Ni-Mo steel by the Sellars model. The Sellars models about the critical conditions for DRX are shown as follows [14]:

$$\varepsilon_c = \mathrm{k}\varepsilon_p \tag{11}$$

$$\varepsilon_c = \mathrm{a}Z^{\mathrm{b}} \tag{12}$$

where k, a and b are material constants; ε_c is the critical strain; ε_p is the peak strain, which can be obtained from the true stress-strain curves.

Based on the DRX kinetic theory, the onset of DRX is dependent on the work hardening rate θ, and the $\ln\theta$-ε curves are fitted and smoothed using a third-order polynomial to obtain the critical strain for DRX[15]. Figure 2 shows the relationship between $-\partial(\ln\theta)/\partial\varepsilon$ and ε at different conditions. From Figure 2, the critical strain for DRX at evaluated temperatures and strains can be calculated.

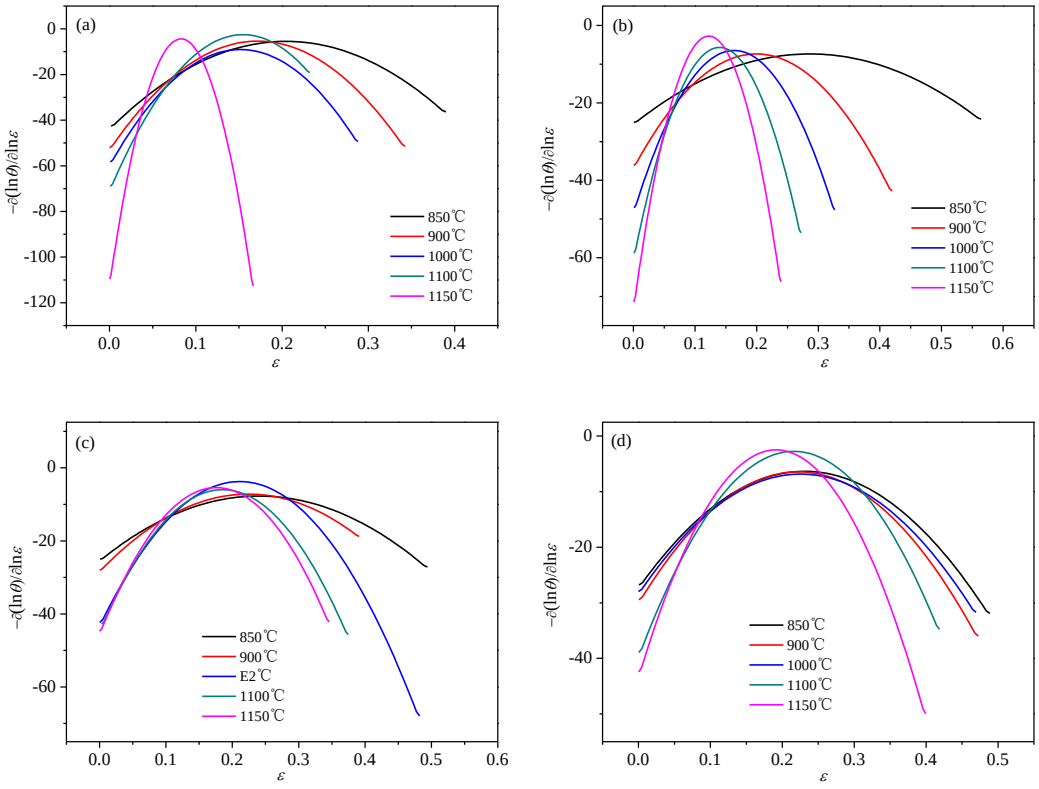

Figure 2. The relationship between $-\partial(\ln\theta)/\partial\varepsilon$ and ε at different strain rate:

(a) 0.01 s^{-1}; (b) 0.1 s^{-1}; (c) 1 s^{-1}; (d) 10 s^{-1}

Meanwhile, by plotting the values of $\ln(\varepsilon_c)$ concerning $\ln(Z)$ and linear regression analysis of 16Cr-5Ni-Mo steel as shown in Figure 3, the dependence of ε_c on Z can be described as:

$$\ln\varepsilon_c = 0.051\ln Z - 3.726 \tag{13}$$

$$\varepsilon_c = 0.024Z^{0.051} \tag{14}$$

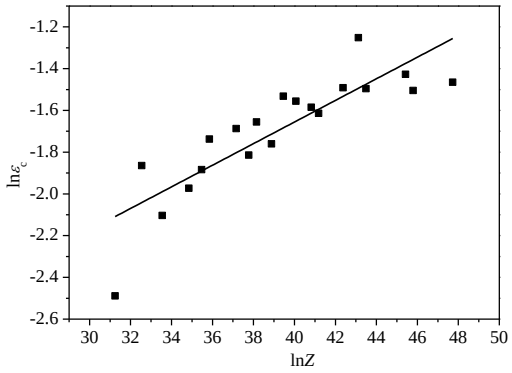

Figure 3. Relationship between ln(Z) and ln(ε_c)

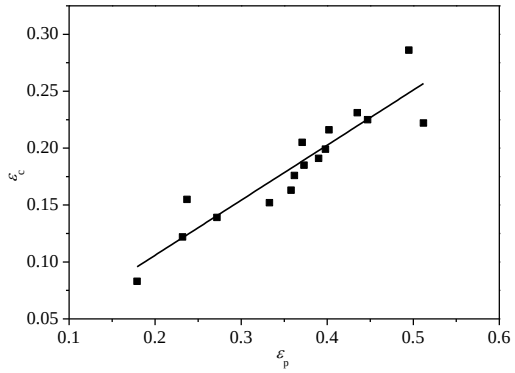

Figure 4. The relationship between the critical strain (ε_c) and peak strain (ε_p)

Based on the values of ε_c and ε_p, the relationship between the critical strain (ε_c) and peak strain (ε_p) can be plotted as shown in Figure 4. And the slope of the fitting line gives the equation in the following:

$$\varepsilon_c = 0.483\varepsilon_p + 0.009 \tag{15}$$

Therefore, the constitutive model for the 16Cr-5Ni-Mo steel considering the DRX can be summarized as follows:

$$\begin{cases} \dot{\varepsilon} = 3.57\times10^{14}[\sinh(0.011\sigma)]^{4.985}\exp(-\dfrac{424173}{RT}) \\ \varepsilon_c = 0.024Z^{0.051} \\ \varepsilon_c = 0.483\varepsilon_p + 0.009 \end{cases}$$

3.3. Processing maps of 16Ni-5Mo-Ni steel

To avoid the hot deformation defects and select the optimal hot working parameters, the method of dynamic material mode (DMM) is often used to establish the processing map. Prasad has developed the DMM which is successfully applied to the research for hundreds of materials [16]. In the DMM, the forging under hot deformation conditions is considered to be a dissipator of power. When the material has enough power to dissipate, the processing conditions are considered to be safe or stable. The total dissipation power P includes G and J, which can be expressed as [17]:

$$p = \sigma\dot{\varepsilon} = G + J = \int_0^{\dot{\varepsilon}} \sigma d\dot{\varepsilon} + \int_0^{\sigma} \dot{\varepsilon} d\sigma \tag{16}$$

where G content is defined as the power dissipated by plastic work; the J content is related to the power dissipated in microstructure evolution.

Based on data of the flow stress, the strain rate sensitivity m can be given in the following equation[18-19]:

$$m = [\frac{\partial(\ln \sigma)}{\partial(\ln \dot{\varepsilon})}]_{\varepsilon T} \tag{17}$$

And the efficiency of power dissipation η given regarding m parameter can be described as follows[20-21]:

$$\eta = \frac{J}{J_{\max}} = \frac{2m}{m+1} \tag{18}$$

The efficiency of power dissipation η is a vital material parameter referring to the power dissipated by metallurgical mechanisms such as the DRX, DRV, wedge cracking, and so on. Consequently, the higher the value of the ηparameter, the better the material dissipates the flow of energy through microstructure evolution. Meanwhile, it means that the material deformed with high ηvalue shows high workability. To display the power dissipation parameters of the steel visually, the three-dimensional (3D) diagrams of the power dissipation efficiency changing with deformation temperature and strain rate are established in Figure. 5 at strains of 0.6 and 0.8, respectively.

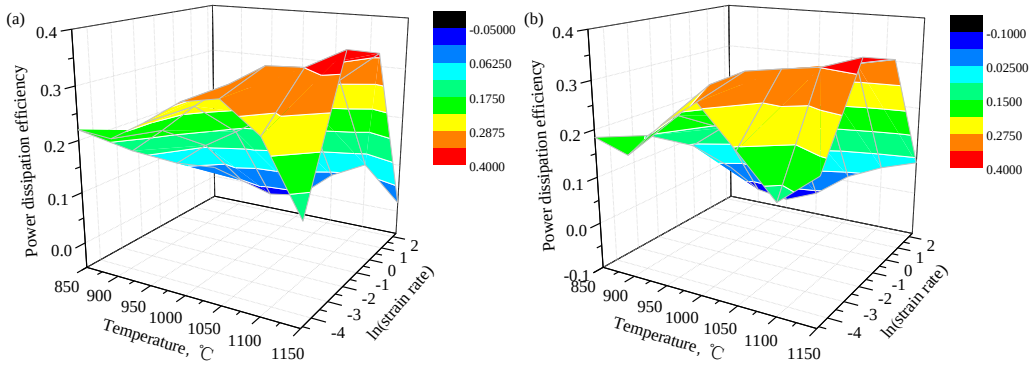

Figure 5. 3D diagrams of power dissipation efficiency of 16Cr-5Ni-Mo steel at strains: (a) 0.6; (b) 0.8

In Figure 5, the power dissipation efficiency is associated with the microstructure evolution, for example, DRX and DRV. Generally, the regions in which the value of power dissipation efficiency is more than 0.3 will be often considered as safe workability. And the conditions of DRX and DRV need a high value of power dissipation. In Figure 5(a), the 3D map displays one region with power dissipation efficiency range of 0.34—0.38 at temperatures of 1050—1150 ℃ and strain rates of 0.02—0.6 s^{-1}. In Figure 5(b), the 3D map displays one region with power dissipation efficiency range of 0.31—0.34 at temperatures of 980—1150 ℃ and strain rates of 0.02—1 s^{-1}. Above regions exhibit high power

dissipation which is usually responding to good workability. However, other defects during hot deformation can also lead to high ηvalue, such as wedge cracking, void formation and so on. Therefore, the ηparameter cannot provide comprehensive advice for hot working. And the parameter ξrepresenting the instability has been considered to determine the workability region for the material. Factor ξ can be expressed as [22-23]:

$$\xi(\dot{\varepsilon}) = \frac{\partial \ln(\frac{m}{m+1})}{\partial \ln(\dot{\varepsilon})} + m < 0 \tag{19}$$

where $\xi(\dot{\varepsilon})$ represents the instability parameter. When the value of $\xi(\dot{\varepsilon})$ is negative, the hot deformation behavior is regarded as instability.

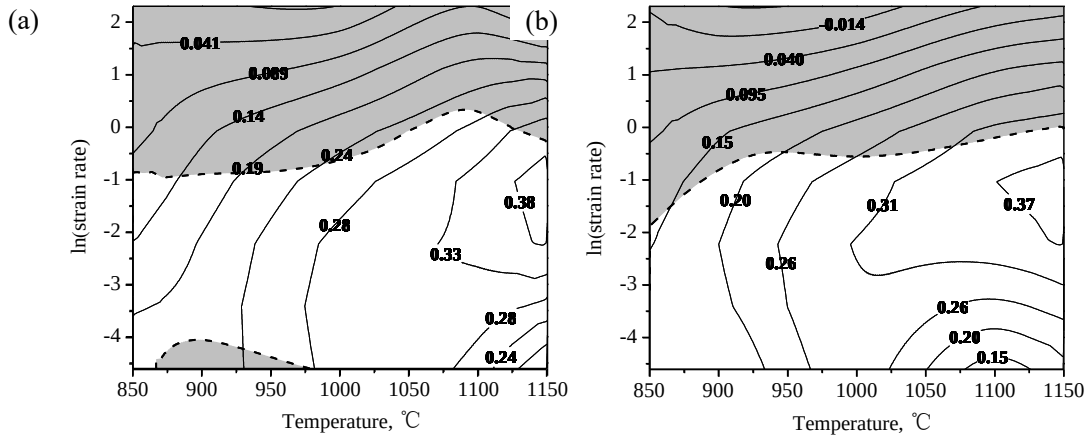

Figure 6. Process maps of 16Cr-5Mo-Ni steel under different temperatures and true strain at strains: (a) 0.6; (b) 0.8

To predict the workability of the 16Cr-5Ni-Mo steel precisely, the processing maps of the steel, composed of power dissipation map and instability map, are drawn in Figure 6. Figures 6(a), (b) show the processing maps at strains of 0.6 and 0.8, respectively. In maps, the contour numbers represent the power dissipation efficiency, and the color regions indicate the flow instability. It can be seen that with increasing of strain, the proportion of flow instability increases. It is pointed out that the variation trend of instability is nearly the same for all the conditions. Due to the considerable deformation strain in the practical production, the strain of over 0.6 is often used which is discussed deliberately in this work. From Figure 6(a) and (b), it can be found that the flow instability occurs at the high deformation strain rate. It is because that at high strain rate, there is not enough time for dislocation slipping and moving, resulting the stress concentration in localized defects and formation of cracking finally. Moreover, at low deformation temperature, such as 850—950 ℃, it also exists the instability region with the low strain rate. For the 16Cr-5Ni-Cr supermartensitic stainless steel, the δ-ferrite appears inevitably. Especially in the deformation, cracking generates along the δ-ferrite as brittle phase easily. Therefore, it should avoid harmful regions during hot working. Based on the processing maps and microstructure evolution, the optimized processing parameters for hot working of 16Cr-5Ni-Mo supermartensitic stainless steel are in the temperature range of 980—1150 ℃ and strain rate range of 0.02—0.36 s^{-1} at

strains of 0.6 and 0.8.

4. Conclusion

(1) For 16Cr-5Ni-Mo steel, the following rate equation by class Arrhenius mode is determined:

$$\dot{\varepsilon} = 3.57 \times 10^{14}[\sinh(0.011\sigma)]^{4.985} \exp(-\frac{424173}{RT})$$

(2) The critical strain for the DRX of 16Cr-5Ni-Mo steel is expressed as: $\varepsilon_c = 0.024Z^{0.051}$ and $\varepsilon_c = 0.483\varepsilon_p + 0.009$, and the equations are used to predict the kinetics of DRX.

(3) Based on DMM, the processing maps of 16Cr-5Ni-Mo steel were established by considering power dissipation maps and instability maps. The optimum domain with high values of power dissipation and without flow instability is in the temperature range of 980—1150 ℃ and strain rate range of 0.02—0.36 s^{-1} at strains of 0.6 and 0.8.

References

[1] Wu G Z, Wang M Q, WANG C F, et al, 2012. *Trans Mater Heat Treat*, **33**(1): 136-40.
[2] Zhong Z Q, Tian Z L, Yang C, et al, 2015. *Eng Fail Analy,* **57**: 129-36.
[3] Ahgaie K M, ADHAMI F, 2010. *Mater. Sci. Eng. A*, **527**: 1052-7.
[4] Zou D N, HAN Y, Yan D N, et al., 2011. *Mater Des*, **32**: 4443-8.
[5] Yuan W H, Gong X H, Sun Y Q, et al., 2016. *J Iron Steel Res Int*, **23**(4): 401-8.
[6] Mirzadeh H, Cabrera J M, Abbas N, 2011. *Acta Mater*, **59**: 6441-8.
[7] Tan Y B, Ma Y H, Zhao F, 2018. *J Alloys Comp*, **741**: 85-96.
[8] Amir H, Mary A W, 2017. *J Mag Alloys*, **5**: 369-87.
[9] Gong B, Duan X W, Liu J S, et al., 2018. *Vacu*, **155**: 345-57.
[10] Meng Q G, Bai C G, Xu D S, 2018. *J Mater Sci Technol*, **34**: 679-88.
[11] Sellars C M, Mctegart W J, 1966. *Acta Metall*, **14:** 1136-8.
[12] Mcqueen H J, Ryan N D, 2002. *Mater Sci Eng A*, **322**(1-2): 43-63.
[13] Zener C, Hollomon J H, 1944. *J Appl Phys*, **15**: 22-32.
[14] Sellars C M, Whiteman J A, 1979. *Metal Sci*, **13**: 187-94.
[15] Najafizadeh A, Jonas J J, 2006. *ISIJ Int*, **46**: 1679-84.
[16] Prasad Y V R K, Gegel H L, Doraivelu S M, et al., 1984. *Metall Mater Trans A*, **15**(10): 1883-92.
[17] Prasad Y V R K, 1990. *India J Technol*, **28**: 435-51.
[18] Gegel H L, Malas J C, Doraivelu S M. *Processing Modeling of P/M Extrusion*. In: G. Bruggeman, V. Weiss (Eds.), Innovations in Materials Processing, Plenum Press, New York, 1985: 137-159.
[19] Liu X G, Ji H P, Guo H, et al., 2013. *Mater Sci Technol*, **29**(1): 24-9.
[20] Venugopal S, Mannan S L, Prasad Y V R K, 1993. *Mater Sci Technol*, **9**: 899-906.
[21] Wan Z P, Hu L X, Sun Y, et al., 2018. *J Alloys Comp*, **769**: 367-75.
[22] Murty S V S N, Rao B N, Kashyap B P, 2000. *Int Mater Rev*, **45**(1): 15-26.
[23] Ren F C, Chen F, Chen J, et al., 2018. *J Manuf Proc*, **31**: 640-9.